Mg/Ca of *Globorotalia inflata* as a recorder of permanent thermocline temperatures in the South Atlantic

Jeroen Groeneveld[1,2] and Cristiano M. Chiessi[1,3]

Received 27 January 2010; revised 18 November 2010; accepted 12 January 2011; published 14 April 2011.

[1] We present a species-specific Mg/Ca-calcification temperature calibration for *Globorotalia inflata* from a suite of 38 core top samples from the South Atlantic (from 8°S to 49°S). *G. inflata* is a deep-dwelling planktonic foraminifer commonly occurring in subtropical to subpolar conditions, which qualifies it for reconstructions of the permanent thermocline. Apparent calcification depths and calcification temperatures were determined by comparing measured δ^{18}O with equilibrium δ^{18}O of calcite based on water column properties. Based on our core top samples, *G. inflata* apparent calcification depth is constant throughout the South Atlantic midlatitudes with a depth of 350–400 m within the permanent thermocline. The resulting Mg/Ca-calcification temperature calibration is Mg/Ca = 0.72 ± 0.045/0.042 exp (0.076 ± 0.006 calcification temperature) (r^2 = 0.81) and covers the temperature range 3.1°C–16.5°C. We applied our Mg/Ca calibration to gravity core PS2495-3 from the Mid-Atlantic Ridge at ~41°S to test its validity by reconstructing a low-resolution record covering the last two glacial-interglacial cycles. Our paleotemperature record reveals large changes in temperature for Terminations I and II, when permanent thermocline temperature increased by as much as 8°C. The *G. inflata* paleotemperature record suggests that oceanic fronts repeatedly migrated over the location of core PS2495-3 during the last 160 kyr. This study shows the potential of *G. inflata* Mg/Ca to reconstruct paleotemperatures in the permanent thermocline.

Citation: Groeneveld, J., and C. M. Chiessi (2011), Mg/Ca of *Globorotalia inflata* as a recorder of permanent thermocline temperatures in the South Atlantic, *Paleoceanography*, *26*, PA2203, doi:10.1029/2010PA001940.

1. Introduction

[2] Over the last decade foraminiferal Mg/Ca has been developed into a powerful proxy to reconstruct marine paleotemperatures [e.g., *Nürnberg et al.*, 1996; *Lea et al.*, 1999; *Mashiotta et al.*, 1999; *Nürnberg et al.*, 2000; *Dekens et al.*, 2002; *Anand et al.*, 2003]. Especially the reconstruction of sea surface temperatures (SST) using Mg/Ca from shallow-dwelling planktonic species has become a routine method. The main advantage of foraminiferal Mg/Ca paleothermometry over other marine paleotemperature proxies is that temperature estimates can be obtained from the same biotic carrier from which oxygen isotopes (δ^{18}O) are obtained. As foraminiferal δ^{18}O is controlled by temperature and δ^{18}O of seawater ($\delta^{18}O_{sw}$), paired Mg/Ca and δ^{18}O measurements on the same sample of foraminiferal calcite are potentially a powerful tool for the reconstruction of $\delta^{18}O_{sw}$ as a proxy for salinity [e.g., *Schmidt et al.*, 2004; *Nürnberg and Groeneveld*, 2006; *Steinke et al.*, 2006; *Came et al.*, 2007].

[3] The application of Mg/Ca paleothermometry to deep-dwelling foraminiferal species, however, has been restricted. There are only a limited number of species-specific Mg/Ca-temperature calibration curves for deep-dwelling species [*Elderfield and Ganssen*, 2000; *Anand et al.*, 2003; *McKenna and Prell*, 2004; *Cléroux et al.*, 2008; *Regenberg et al.*, 2009]. Yet, deep-dwelling foraminifera constitute potential recorders of thermocline conditions [*Fairbanks et al.*, 1982; *Cléroux et al.*, 2007], and hence provide useful information on the upper ocean's stratification and thermal capacity.

[4] *Globorotalia inflata* is one of the most abundant deep-dwelling transitional water species in the South Atlantic [e.g., *Bé and Hutson*, 1977; *Niebler and Gersonde*, 1998]. Its occurrence in core top samples amounts to >20% of the total planktonic foraminiferal assemblage between 30 and 50°S, encompassing the Subtropical Front (STF) and Subantarctic Front (SAF) as well as part of the Polar Frontal Zone (PFZ). During its ontogenetic cycle, *G. inflata* migrates through the upper few hundred meters of the water column [e.g., *Lončarić et al.*, 2006; *Wilke et al.*, 2006; *Chiessi et al.*, 2007; *Cléroux et al.*, 2007], providing great potential of recording past thermocline conditions [*Chiessi et al.*, 2008] as well as the migration of midlatitude oceanic fronts.

[1]MARUM-Center for Marine Environmental Sciences, University of Bremen, Bremen, Germany.
[2]Now at Marum Excellence Cluster, Alfred Wegener Institute for Polar and Marine Research, Bremerhaven, Germany.
[3]Now at School of Arts, Sciences and Humanities, University of São Paulo, São Paulo, Brazil.

0883-8305/11/2010PA001940

[5] In this study we present a Mg/Ca-calcification temperature calibration for *G. inflata* that we derive from core top samples from the South Atlantic. Additionally, we compare Mg/Ca of specimens from different size fractions and different states of encrustation to demonstrate the impact of encrustation on Mg/Ca. We test our calibration on a downcore *G. inflata* Mg/Ca record from gravity core PS2495-3 raised in the Subantarctic Zone (SAZ) of the Mid-Atlantic Ridge to assess the migration of the STF and the SAF during the last two glacial-interglacial cycles. Our data show that Mg/Ca from *G. inflata* is a reliable recorder of permanent thermocline temperatures even under considerably different upper water column structures, highlighting its applicability in paleoceanographic studies.

2. Materials and Methods

2.1. Samples

[6] We used a set of 38 core top samples from the South Atlantic that were retrieved between 8°S and 49°S, 6°E and 60°W, covering water depths between ~500 and 3800 m (Figure 1a and Table 1) to establish our Mg/Ca-calcification temperature calibration for *G. inflata*. For the determination of the apparent calcification depth of *G. inflata* we also included 22 additional core top samples from the western South Atlantic already published by *Chiessi et al.* [2007].

[7] Samples were taken from the undisturbed uppermost centimeter of multicores. The late Holocene age of all samples was confirmed by the presence of stained benthic foraminifera [*Harloff and Mackensen*, 1997; *Chiessi et al.*, 2007; this study]. Additionally, isotope stratigraphy for core GeoB2109-3 [*Dürkoop*, 1998], and AMS ^{14}C ages for cores GeoB2804-2 and GeoB2805-1 (0 years BP [*Mollenhauer et al.*, 2006]) corroborate the late Holocene age of the samples.

[8] To test the application of our *G. inflata* Mg/Ca-calcification temperature calibration Mg/Ca analyses were performed on gravity core PS2495-3 (41.27°S, 14.49°W, 3134 m water depth), raised from the eastern slope of the Mid-Atlantic Ridge (Figure 1a). This test case application is meant to test and demonstrate the feasibility of our approach to reliably reconstruct permanent thermocline temperatures. The core is located between the modern STF (38–42°S) and SAF (~45°S) [*Peterson and Stramma*, 1991; *Tsuchiya et al.*, 1994], providing the opportunity to test our new Mg/Ca calibration by assessing the temperature effects associated with migrations of these oceanic features. The original age model of core PS2495-3 is based on 10 calibrated AMS ^{14}C dates for the last ~30 kyr [*Gersonde et al.*, 2003] and on standard oxygen isotope stratigraphy on the benthic foraminifer *Cibicidoides spp.* [*Mackensen et al.*, 2001]. For this study we further tuned the original age model of PS2495-3 to the global benthic δ^{18}O stack of *Lisiecki and Raymo* [2005]. All data presented here are stored in the Pangaea data bank (www.pangaea.de), including the old and new age models.

2.2. Selection of *G. inflata* Size Fraction and Morphology

[9] Although maximum abundances of *G. inflata* often occur within the thermocline [e.g., *Fairbanks et al.*, 1982], calcification of the tests takes place from the mixed layer to water depths possibly deeper than 500 m [e.g., *Wilke et al.*, 2006]. Accordingly, the tests integrate the hydrographic signals in their proxy data that they acquired over a considerable range of water depths. Moreover, sediment samples often contain a large variety in morphology of individual *G. inflata* specimens, that is, from small, juvenile *G. inflata* to heavily encrusted and much larger specimens (Figure 2). This provides a potential source of bias when using proxies like Mg/Ca. Therefore, we selected only nonencrusted specimens of *G. inflata* with three chambers in the final whorl [*Kennett and Srinivasan*, 1983] in the size range 315–400 μm for the establishment of both the Mg/Ca-calcification temperature calibration and the downcore record. We define nonencrusted specimens as those specimens which are not covered by a shiny calcite crust when observed under a binocular microscope. However, SEM analyses showed that even these specimens do contain some calcite crust (Figure 2). To determine the bias introduced on downcore temperature reconstructions when specimens of different size and morphology are mixed, we also analyzed three additional size fractions of nonencrusted specimens (<250 μm, 250–315 μm, and >400 μm) as well as heavily encrusted, shiny specimens (315–400 μm) from four core depths (Holocene, MIS2, MIS5, and MIS6).

2.3. Mg/Ca and Stable Oxygen Isotope Analyses

[10] Between 20 and 50 tests of *G. inflata* were selected from the different size fractions from each sample and gently crushed. The shell fragments were then cleaned according to the standard cleaning protocol for foraminiferal Mg/Ca analyses [*Barker et al.*, 2003]. The tests underwent ultrasonic cleaning alternated with washes in deionized water (Seralpur) and methanol, before an oxidizing step was applied, which was neutralized with multiple deionized water washes (Seralpur). After transfer into clean vials a weak acid leach (0.001 M QD HNO_3) was applied, and samples were dissolved in 0.075 M QD HNO_3. Before dilution samples were centrifuged for 10 min (6000 rpm) to exclude any remaining insoluble particles from the analyses. Samples were diluted with Seralpur water before analysis with an ICP-OES (Perkin Elmer Optima 3300RL with autosampler and ultrasonic nebulizer U-5000 AT (Cetac Technologies Inc.)) at the Department of Geosciences, University of Bremen. Instrumental precision of the ICP-OES was monitored by analysis of an in-house standard solution with a Mg/Ca of 2.93 mmol/mol after every five samples (long-term standard deviation of 0.026 mmol/mol or 0.91%). To allow interlaboratory comparison we analyzed an international limestone standard (ECRM752–1) with a reported Mg/Ca of 3.75 mmol/mol [*Greaves et al.*, 2008]. The long-term average of the ECRM752–1 standard, which was routinely analyzed twice before each batch of 50 samples in every session, is 3.78 mmol/mol (1σ = 0.066 mmol/mol). Analytical precision based on three replicate measurements of each sample for *G. inflata* was 0.23% for Mg/Ca, while reproducibility of the samples (n = 47; separately cleaned and analyzed during different ICP-OES sessions) was ±0.12 mmol/mol (1σ, ~3.8%).

[11] Stable oxygen isotope ratios were determined on the same samples analyzed for Mg/Ca. We measured between 5 and 15 specimens of *G. inflata*, depending on the size fraction. Specimens were picked together and then separated

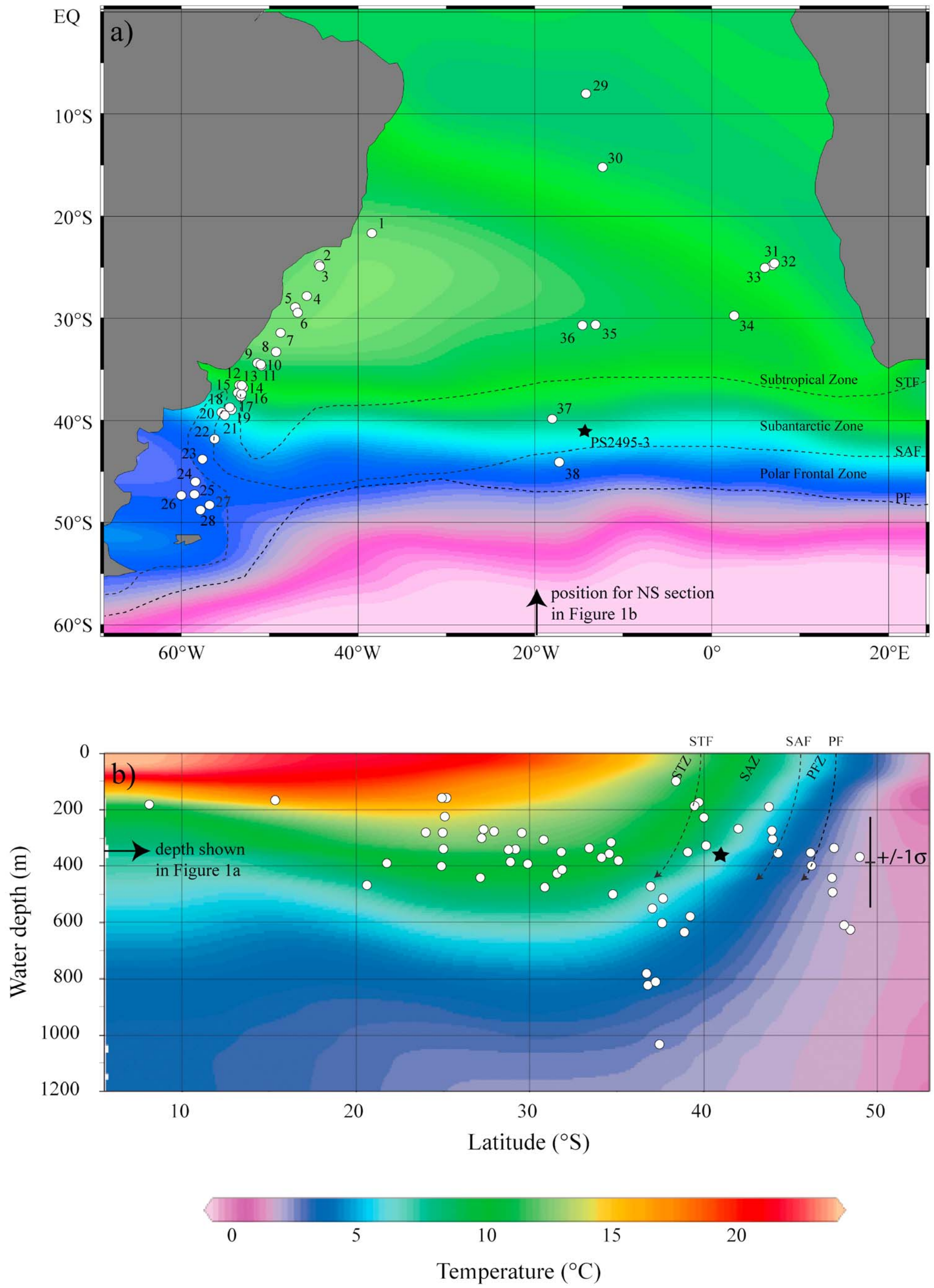

Figure 1. (a) Map with surface sample locations (white circles; numbers refer to Table 1), showing mean annual temperature at 350 m water depth [*Locarnini et al.*, 2006]. The position of gravity core PS2495-3 is indicated by the black star. The black arrow depicts the position of the N-S cross section shown in Figure 1b. Dashed lines indicate the position of the Subtropical Front (STF), the Subantarctic Front (SAF), and the Polar Front (PF) at the sea surface [*Peterson and Stramma*, 1991]. (b) Cross section from 5°S to 55°S at 20°W in the South Atlantic showing mean annual temperatures down to a water depth of 1200 m [*Locarnini et al.*, 2006]. White circles indicate *G. inflata* apparent calcification depth at the location of the core top samples used in this study based on foraminiferal δ^{18}O analyses. The black star indicates the position of gravity core PS2495-3 at the apparent calcification depth of *G. inflata*. The black arrow depicts the depth of the temperatures shown in Figure 1a. Dashed lines indicate the mean position of the STF, the SAF, and the PF that mark the Subtropical Zone (STZ), the Subantarctic Zone (SAZ), and the Polar Frontal Zone (PFZ) [*Peterson and Stramma*, 1991]. The vertical black bar depicts the error ($\pm 1\sigma$) on the estimation of *G. inflata* apparent calcification depth.

Table 1. Surface Sample Locations, *G. inflata* δ^{18}O, Mg/Ca, Apparent Calcification Depths, and Calcification Temperatures[a]

Sample Code in Figure 1	Site (GeoB)	Latitude (°S)	Longitude (°E)	Water depth (m)	δ^{18}O[b] (‰ VPDB)	Mg/Ca (mmol/mol)	Apparent Calcification Depth[c] (m)	Calcification Temperature[d] (°C)
1	2119-2	21.73	−38.55	2958	1.17	2.34	391	12.32
2	6908-1	24.86	−44.52	500	1.47	2.25	399	11.25
3	6909-2	24.98	−44.44	1032	1.24	1.85	338	12.58
4	2109-3	27.91	−45.87	2513	0.71	2.01	278	14.86
5	6202-5	29.09	−47.17	1493	0.87	1.46	341	13.27
6	6205-1	29.50	−46.92	2004	0.71	2.19	283	14.69
7	6210-1	31.52	−48.82	2499	0.92	1.87	426	12.90
8	6220-1	33.36	−49.39	2277	0.75	2.22	335	14.11
9	6214-5	34.53	−51.44	1567	0.94	1.98	356	12.72
10	6216-1	34.62	−51.23	2032	0.77	1.76	315	13.64
11	6217-2	34.72	−51.00	2399	1.54	1.47	499	9.57
12	6234-1	36.69	−53.46	1140	2.43	0.82	780	4.16
13	6233-1	36.75	−53.30	1627	2.57	0.77	824	3.69
14	6232-1	36.90	−53.14	2560	1.44	1.06	472	7.43
15	2803-1	37.41	−53.71	1162	2.97	1.02	1033	3.34
16	2804-2	37.54	−53.53	1836	2.27	1.27	602	5.64
17	2805-1	37.61	−53.44	2759	2.13	1.13	516	6.76
18	6311-2	38.81	−54.63	996	2.73	1.10	635	4.25
19	6310-1	39.04	−54.32	1455	2.65	0.93	352	5.67
20	6313-2	39.42	−55.44	733	2.67	0.95	179	4.99
21	6314-2	39.64	−55.15	1187	2.65	1.21	176	5.03
22	2707-4	41.94	−56.32	3167	2.97	0.98	267	3.82
23	2715-1	43.91	−57.66	3277	2.90	0.87	304	3.48
24	6334-2	46.09	−58.52	2597	2.88	1.03	354	3.47
25	2722-2	47.33	−58.62	2383	2.93	0.92	493	3.35
26	2719-2	47.44	−60.09	684	2.76	0.97	336	4.33
27	2726-3	48.39	−56.93	1405	3.03	1.35	627	3.12
28	2723-2	48.91	−57.88	569	2.79	1.21	368	3.88
29	5002-2	8.08	−14.32	2849	0.98	2.66	180	13.27
30	1417-2	15.31	−12.42	2845	0.43	2.53	167	16.52
31	1216-2	24.93	6.79	2263	1.23	2.30	280	11.63
32	1217-1	24.95	6.73	2007	0.69	2.38	156	14.57
33	1218-1	25.17	5.92	1023	0.64	2.22	158	14.87
34	1728-3	29.84	2.41	2887	1.35	1.30	392	10.96
35	3807-1	30.75	−13.20	2515	0.90	1.99	306	13.41
36	3808-7	30.81	−14.71	3213	1.44	1.82	476	10.33
37	6416-2	39.95	−18.16	3525	1.40	1.59	227	10.75
38	6413-4	44.21	−17.34	3768	2.55	0.82	353	4.82
39	2130-1	20.62	−37.10	2113	1.51	n.a.	468	10.24
40	2102-1	23.98	−41.20	1805	0.73	n.a.	280	15.47
41	6911-2	25.09	−44.37	1604	0.63	n.a.	225	15.92
42	2106-1	27.10	−46.50	502	1.28	n.a.	442	11.31
43	2107-5	27.18	−46.46	1052	0.80	n.a.	300	14.22
44	2104-1	27.29	−46.38	1505	0.70	n.a.	270	14.85
45	6204-2	28.71	−47.37	578	1.00	n.a.	342	12.73
46	6203-1	28.83	−47.30	1001	1.13	n.a.	384	11.84
47	6209-2	31.76	−48.15	3013	0.73	n.a.	349	14.30
48	6208-1	31.81	−45.66	3693	1.07	n.a.	412	12.58
49	6222-2	34.08	−48.62	3450	1.08	n.a.	369	12.55
50	6218-1	35.05	−50.78	2953	1.10	n.a.	381	12.01
51	6231-1	36.99	−53.02	2955	1.69	n.a.	550	6.26
52	2802-2	37.21	−53.98	1007	2.61	n.a.	811	4.02
53	6312-1	38.35	−55.26	435	2.40	n.a.	95	6.69
54	6309-2	39.17	−54.15	2869	2.90	n.a.	577	4.04
55	6317-2	40.08	−54.60	3115	2.71	n.a.	327	5.68
56	2712-1	43.68	−59.33	1228	2.73	n.a.	189	3.89
57	2714-5	43.86	−58.00	2361	2.87	n.a.	274	3.57
58	6336-2	46.14	−57.85	3398	2.91	n.a.	399	3.37
59	2718-1	47.31	−58.18	2990	2.88	n.a.	443	3.48
60	2727-1	48.01	−56.54	2803	3.01	n.a.	610	3.17

[a]Samples 39–60 are from *Chiessi et al.* [2007].
[b]Analyzed on *G. inflata.*
[c]Based on comparison of $\delta^{18}O_{G.\ inflata}$ and equilibrium δ^{18}O profiles calculated for every sample site with temperatures from the World Ocean Atlas 2005 [*Locarnini et al*., 2006], seawater δ^{18}O from *LeGrande and Schmidt* [2006], and the paleotemperature equation of *Shackleton* [1974].
[d]From the World Ocean Atlas 2005 [*Locarnini et al.*, 2006] for each surface sample location at its respective apparent calcification depth.

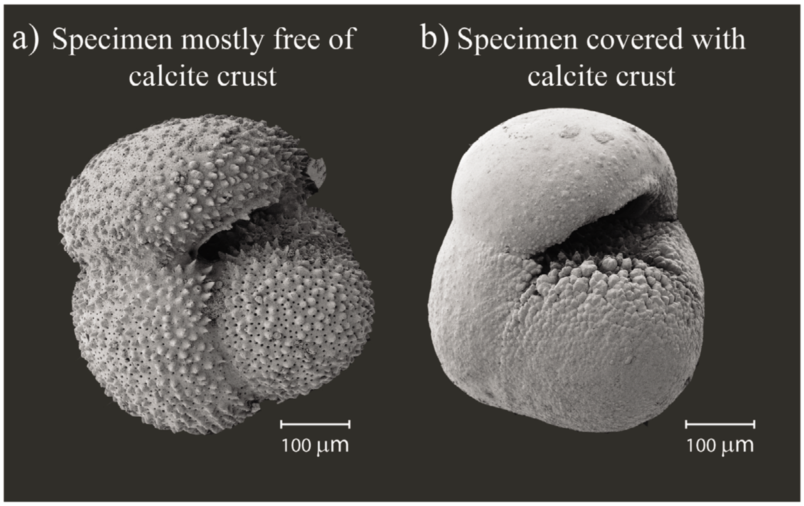

Figure 2. Scanning electron microscope (SEM) images of characteristic *G. inflata* tests from gravity core PS2495-3 classified as (a) nonencrusted and (b) encrusted specimens. Imaging was performed at the Department of Geosciences, University of Bremen.

for either Mg/Ca or stable oxygen isotope analysis. Stable oxygen isotope analyses were performed using a Finnigan MAT 251 mass spectrometer with an automated carbonate preparation device at the Department of Geosciences, University of Bremen. The external standard error of the stable oxygen isotope analyses is <0.06‰. Values are reported relative to the Vienna Pee Dee Belemnite (VPDB), calibrated by using the National Bureau of Standards (NBS) 18, 19, and 20 standards.

2.4. Determination of Calcification Temperatures

[12] We determined calcification temperatures based on measured δ^{18}O of *G. inflata*. As deep-dwelling foraminifera like *G. inflata* have a much larger habitat range than shallow-dwelling foraminifera, it is necessary to first calculate calcification temperatures in order to construct a Mg/Ca-calcification temperature calibration. We first calculated the equilibrium δ^{18}O of calcite ($\delta^{18}O_{equ}$) for the whole water column above each surface sample location. For this we used mean annual temperatures from the World Ocean Atlas 2005 [*Locarnini et al.*, 2006], $\delta^{18}O_{sw}$ from the global gridded data set of *LeGrande and Schmidt* [2006], and the paleotemperature equation from *Shackleton* [1974]. One $\delta^{18}O_{equ}$ depth profile was generated for each surface sample site based on the closest grid point from the *Locarnini et al.* [2006] and *LeGrande and Schmidt* [2006] databases. The $\delta^{18}O_{equ}$ profiles have been calculated for all depth levels of the World Ocean Atlas 2005 down to 1500 m. As no species-specific paleotemperature equation is available for *G. inflata* we chose the equation of *Shackleton* [1974] since (1) the apparent calcification disequilibrium is relatively small (0 ± 0.3‰) for deep-dwelling foraminiferal species [*Fairbanks et al.*, 1982; *Deuser and Ross*, 1989; *Wilke et al.*, 2006] and (2) it correctly predicts the slope of the δ^{18}O – temperature relationship over the entire temperature range present in the oceans for the most commonly used species of planktonic foraminifera [*Mulitza et al.*, 2003]. In a second step, we determined the apparent calcification depth by comparing foraminiferal δ^{18}O with the $\delta^{18}O_{equ}$ profiles (Table 1). Finally, we obtained the calcification temperature (Table 1) from the World Ocean Atlas 2005 [*Locarnini et al.*, 2006] for each surface sample location at its respective apparent calcification depth.

3. Results

3.1. Calcification Temperatures

[13] The stable oxygen isotope composition of *G. inflata* from core top samples varies between 0.43 and 3.03‰ (Table 1). Apparent calcification depths are between 95 and 1033 m with a mean value of 387 m (1σ = 179 m), and calcification temperatures vary between 3.1°C and 16.5°C (Figure 1b and Table 1).

[14] The spread in apparent calcification depths is highest close to the STF (38–42°S) in the area of the Brazil-Malvinas Confluence (BMC; westernmost South Atlantic). At the BMC the Brazil Current meets the Malvinas (Falkland) Current, resulting in a highly energetic area with frequent formation of eddies [*Olson et al.*, 1988; *Stramma and England*, 1999]. The resulting strong currents and large-scale eddies can carry planktonic foraminifera away from their natural habitat. Such expatriation may play an important role in the Brazil-Malvinas Confluence [*Berger*, 1970; *Bijma et al.*, 1990; *Boltovskoy*, 1994]. Expatriated foraminifera often survive and keep calcifying at water depth ranges that are outside their typical habitat depth [*Boltovskoy*, 1994]. As a result of the expatriation their apparent calcification depth and calcification temperature will differ from that observed under typical conditions. Nevertheless, the resulting Mg/Ca versus calcification temperature pair will be a realistic combination, and can be used in the calibration. Additionally, the position of the BMC shows significant variation over the year, so that it is reasonable to consider a seasonality effect as contributing further to the large scatter seen in the BMC core top database [e.g., *Olson et al.*, 1988]. The location of core PS2495-3 is under open-ocean conditions at

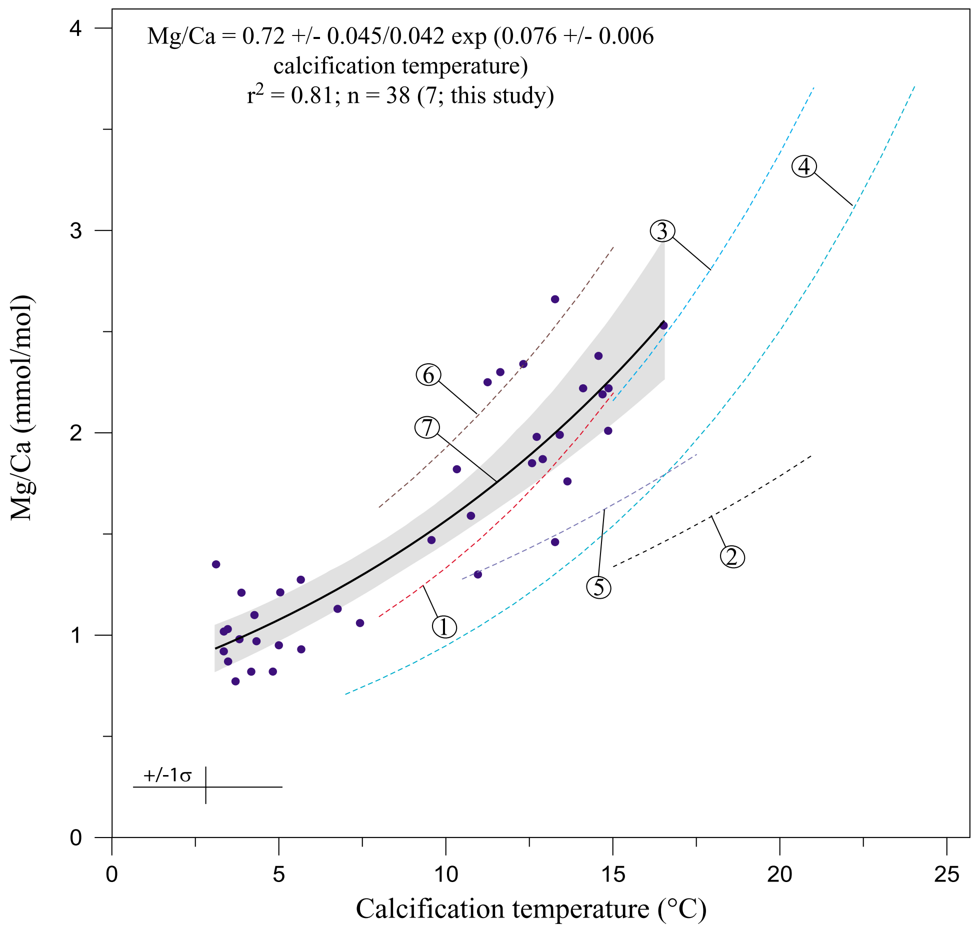

Figure 3. Mg/Ca and calcification temperatures for *G. inflata* core top samples (blue dots) covering the temperature range 3.1°C–16.5°C. For comparison, existing Mg/Ca-temperature calibrations for *G. inflata* and other deep-dwelling planktonic foraminifera are shown. The numbers refer to Table 2, where the details of the different Mg/Ca-temperature calibrations are given. The black cross depicts the errors (±1σ) associated with uncertainties in the determination of apparent calcification depths and in Mg/Ca analyses reflecting analytical and biological variation. The grey shaded area enveloping our calibration curve reflects the 99% confidence interval of the regression curve, based on the errors of the coefficients A and B of our calibration. Our Mg/Ca-calcification temperature calibration is also given in numerical form.

the Mid-Atlantic Ridge, rather than near the BMC, so that expatriation is not an issue for our downcore record.

3.2. Mg/Ca-Calcification Temperature Calibration

[15] Mg/Ca of *G. inflata* core top samples varies between 0.77 and 2.66 mmol/mol (Table 1). These ratios were combined with their respective calcification temperatures to derive the following exponential Mg/Ca-calcification temperature calibration equation (Figure 3):

$$\mathrm{Mg/Ca} = 0.72\ \exp(0.076\,\text{calcification temperature}),\ r^2 = 0.81 \quad (1)$$

with Mg/Ca in mmol/mol and δ^{18}O-derived calcification temperatures in degrees Celsius. The regression curve is defined by the slope 0.076 (or A in general exponential regression curves) which is the temperature-sensitive component, and the *y* axis intercept 0.72 (or B in general exponential regression curves). The standard errors of the parameter estimates are ±0.006 for A and +0.045 and −0.042 for B.

[16] Apart from the small analytical errors which were presented in section 2.3., a significant uncertainty affecting the precision of temperature reconstructions based on equation (1) is related to the considerable spread in δ^{18}O-derived calcification temperatures. We estimated an error of 2.25°C as the standard deviation from the residuals between calcification temperatures and temperatures calculated from equation (1). The standard deviation in temperature reconstructions based on equation (1) is significantly higher than error estimates for shallow-dwelling planktonic foraminifera of 1–1.5°C [e.g., *Lea et al.*, 1999; *Dekens et al.*, 2002; *Anand et al.*, 2003] but in agreement with previously published calibrations for deep-dwelling foraminifera [*McKenna and Prell*, 2004; *Cléroux et al.*, 2008; *Regenberg et al.*, 2009]. This difference is most likely due to a combination of the following factors: (1) the variable depth range and, hence, conditions under which deep-dwelling

planktonic foraminifera calcify; (2) the formation of a calcite crust typical for most deep-dwelling species, which will be present in different proportions depending on location or sample preservation; and (3) the uncertainties related to the estimation of apparent calcification depth (e.g., the choice of the paleotemperature equation used for $\delta^{18}O_{equ}$, influence of expatriation specifically at the location of the BMC, and possible foraminiferal δ^{18}O-disequilibrium effects).

[17] Recently, the potential influence of salinity on foraminiferal Mg/Ca has received significant attention [*Kisakürek et al.*, 2008; *Ferguson et al.*, 2008; *Groeneveld et al.*, 2008; *Hoogakker et al.*, 2009; *Sadekov et al.*, 2009]. It has been shown that especially under high-salinity conditions like in the Caribbean, Mediterranean, and the Red Sea with salinities reaching up to 40 psu the influence is significant [*Ferguson et al.*, 2008; *Hoogakker et al.*, 2009]. Subsurface (~350 m water depth) salinity in the South Atlantic is ~35 psu north of the STF, whereas salinity decreases to ~34 psu south of the SAF [*Locarnini et al.*, 2006]. We estimate the impact of salinity on Mg/Ca at our core site to be equivalent to a Mg/Ca temperature signal of ~1°C [*Kisakürek et al.*, 2008].

3.3. PS2495-3 Downcore Record

[18] *G. inflata* Mg/Ca from gravity core PS2495-3 varies between 0.92 and 2.11 mmol/mol, which translates into a temperature range of between 2.9°C and 14.0°C (Figure 4). Terminations I and II are represented by large temperature changes of ~8°C. Transitions from MIS5 to MIS4 and from MIS3 to MIS2 show sharp decreases in Mg/Ca from 1.43 to 0.95 mmol/mol and from 1.20 to 0.93 mmol/mol, respectively. These steps correspond to temperature changes of 5.5°C and 3.5°C, respectively. The *G. inflata* δ^{18}O values range between 0.82‰ and 3.61‰ (Figure 4). Highest values occur during MIS2 and MIS4, when Mg/Ca is at a minimum. As temperature changes are as large as 8°C, the δ^{18}O record is dominated by changes in temperature overruling changes in salinity. The Mg/Ca record and derived paleotemperatures will be used below in conjunction with an independent temperature estimator to test the feasibility of our calibration.

4. Discussion

4.1. South Atlantic *G. inflata* Apparent Calcification Depth and Mg/Ca-Calcification Temperature Calibration

[19] The apparent calcification depth of *G. inflata* from the South Atlantic calculated for nonencrusted specimens from the 315–400 μm fraction is 387 ± 179 m. Plankton tow studies performed off southwest Africa [*Lončarić et al.*, 2006; *Wilke et al.*, 2006] showed that *G. inflata* occurs over a wide range of water depths with maximum abundance in the thermocline. Based on *G. inflata* δ^{18}O values *Lončarić et al.* [2006] showed that calcification also occurs over a large range of water depths with a mean apparent calcification depth of ~250 m. *Elderfield and Ganssen* [2000] assigned an apparent calcification depth for *G. inflata* of 300–400 m, based on core tops from the North Atlantic.

[20] In contrast to these findings, *Cléroux et al.* [2007] showed after analyzing a collection of core tops from the North Atlantic that *G. inflata* mainly records conditions at the base of the seasonal thermocline (<100 m) and only descends deeper in the water column when temperatures at that depth are above 16°C. One explanation for this apparent discrepancy is that *G. inflata* occupies a different depth habitat in the North Atlantic in comparison with the South Atlantic [*Bé and Tolderlund*, 1971]. But, this does not explain the differences between the results of *Cléroux et al.* [2007] and *Elderfield and Ganssen* [2000] that are both based on North Atlantic samples. A potential explanation for this difference could be a different encrustation state of the analyzed specimens, which was not included in these studies. This apparent disagreement between different studies suggests the importance of defining a clear and narrow state of encrustation of the *G. inflata* specimens to be used for proxy analyses.

[21] *Elderfield and Ganssen* [2000], *Anand et al.* [2003], and *Cléroux et al.* [2008] already reported Mg/Ca measurements on recent *G. inflata* specimens (Figure 3 and Table 2) from the North Atlantic. Our calibration is very similar to the one of *Elderfield and Ganssen* [2000] and to the one in which the slope was fixed at 0.09 [*Anand et al.*, 2003] extending the Mg/Ca calibration to colder temperatures by ~5°C. The comparison of our equation with the calibrations of *Cléroux et al.* [2008] and of *Anand et al.* [2003] in which the slope was not fixed, however, shows significant dissimilarities. The calibrations from *Cléroux et al.* [2008] and *Anand et al.* [2003] not only show a lower temperature dependency than our equation but the absolute Mg/Ca is offset from ours by 0.7–1.0 mmol/mol at a temperature of 15°C. These differences could also be related to the possible existence of different genetic types of *G. inflata* for the North and the South Atlantic. Different genetic types have been determined for many planktonic foraminiferal species [*Darling and Wade*, 2008, and references therein]. Although only one genetic type of *G. inflata* is known yet [*de Vargas et al.*, 1997], different genetic types for another Globorotalia species, *Globorotalia truncatulinoides*, have been described [*de Vargas et al.*, 2001]. Also, for *Neogloboquadrina pachyderma* different genetic types for the North and South Atlantic were determined [*Darling et al.*, 2004].

[22] Further comparison with Mg/Ca calibration equations for other deep-dwelling planktonic foraminifera, such as *G. truncatulinoides* and *Globorotalia crassaformis*, shows a roughly similar picture, although differences are present in absolute values, presumably pointing to interspecies differences and varying states of encrustation (Figure 3) [*McKenna and Prell*, 2004; *Regenberg et al.*, 2009].

4.2. Potential Bias Caused by Different Size Fractions and States of Encrustation

[23] As *G. inflata* calcifies over a large depth range, Mg/Ca represents an average signal over this depth range. As the specimens descend through the water column they also acquire a calcite crust recording lower temperatures than the primary calcite. Hence, larger specimens are expected to contain a larger portion of calcite crust and lower Mg/Ca. *Hathorne et al.* [2009] showed for *G. inflata* specimens from a North Atlantic sediment trap that Mg/Ca of the primary calcite is 2–3 times higher than the calcite crust. *Cléroux et al.* [2008], on the other hand, analyzed two different size fractions of *G. inflata*, 250–315 μm and

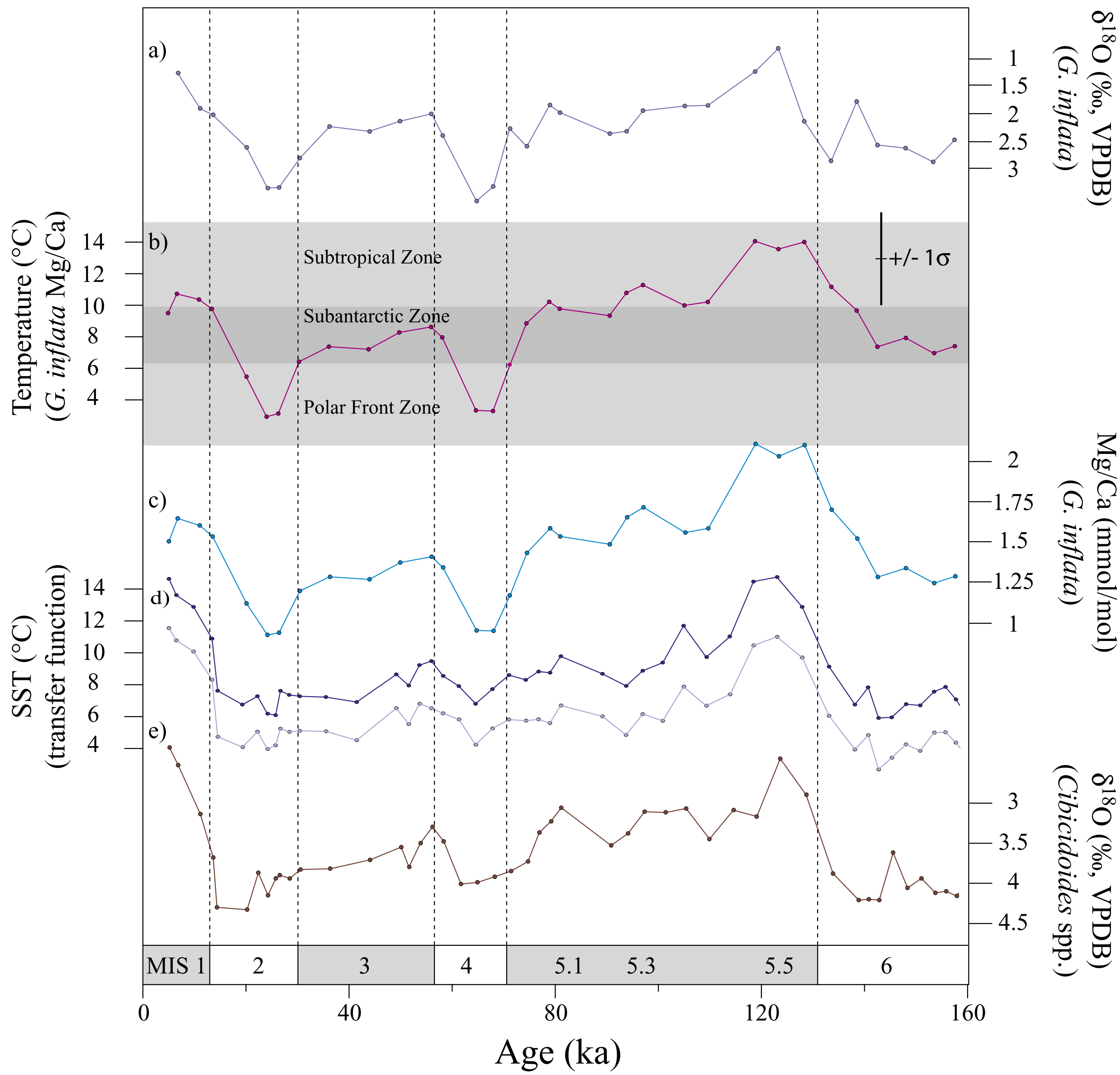

Figure 4. Downcore records from gravity core PS2495-3 covering the last 160 kyr. (a) *G. inflata* δ^{18}O. (b) *G. inflata* Mg/Ca paleotemperatures. (c) *G. inflata* Mg/Ca. (d) Summer and winter sea surface temperatures based on foraminiferal transfer functions [*Gersonde et al.*, 2004]. (e) *Cibicidoides spp*. δ^{18}O [*Mackensen et al.*, 2001]. Horizontal grey shaded bars in Figure 4b give a possible indication when core PS2495-3 was located in the Subtropical Zone, Subantarctic Zone, or Polar Frontal Zone [*Peterson and Stramma*, 1991]. Numbers on the lower portion of the plot depict Marine Isotope Stages (MIS), and vertical dashed lines mark the boundaries between adjacent stages. The vertical black bar in Figure 4b depicts the error ($\pm 1\sigma$) associated with our Mg/Ca-calcification temperature calibration equation.

355–400 μm, indicating that no significant difference in Mg/Ca was present between both size fractions.

[24] In this study we extended the range of size fractions to detect potential biases in Mg/Ca, though always selecting specimens with the same state of encrustation (defined as nonencrusted) as used for the calibration. Additionally, we also included samples with heavily encrusted, shiny specimens. An increase in size fraction is systematically related to a decrease in Mg/Ca (Figure 5). Mg/Ca in specimens <250 μm is warmer (2.0°C on average) than the nonencrusted 315–400 μm specimens. Mg/Ca from the 250–315 μm fraction (+0.7°C) is most similar to the 315–400 μm fraction, which is in agreement with *Cléroux et al.* [2008]. Lowest Mg/Ca is recorded by the largest specimens (>400 μm) and heavily encrusted specimens, which deviate 2.2°C and 4.4°C, respectively, from the fraction used for our

Table 2. Mg/Ca-Temperature Calibration Equations for Several Deep-Dwelling Foraminifera, Source of the Analyzed Foraminifera, Size Fractions, and Temperature Range of the Calibrations

Species	Curve Code in Figure 3	Source	Size Fraction (μm)	A[a]	B[a]	r^2	Temperature Range (°C)	Reference
G. inflata	1	surface samples	n.a.	0.49	0.10	n.a.	7.5–15	*Elderfield and Ganssen* [2000]
G. inflata	2	sediment trap	350–500	0.56	0.058	0.55	15–21	*Anand et al.* [2003]
G. inflata	3	sediment trap	350–500	0.299	0.09	n.a.	15–21	*Anand et al.* [2003]
G. truncatulinoides (dextral)	4	surface samples	n.a.	0.355	0.098	0.92	7–23	*McKenna and Prell* [2004]
G. inflata	5	surface samples	355–400	0.71	0.06	0.72	10.5–17.9	*Cléroux et al.* [2008]
G. truncatulinoides/G. crassaformis	6	surface samples	355–400	0.84	0.083	0.72	8–15	*Regenberg et al.* [2009]
G. inflata	7	surface samples	315–400	0.72[b]	0.076[b]	0.81	3.1–16.5	this study

[a]A is the temperature-sensitive component and B is the *y* axis intercept in the general exponential expression Mg/Ca = B*exp(A*temperature).
[b]The standard errors of the parameter estimates are ±0.006 for A, and +0.045 and −0.042 for B.

calibration equation (315–400 μm). This experiment suggests that with increasing size the proportion of calcite crust increases, which was also shown for several other planktonic foraminifer species [*Caron et al.*, 1990] indicating that the specimens calcified a larger fraction of the total test mass deeper in the water column. Therefore, their average chemical signature represents deeper conditions in the water column if compared to smaller, nonencrusted specimens. We state that careful and consistent selection concerning size and state of encrustation of specimens of *G. inflata* is essential for a reliable reconstruction of paleotemperatures.

[25] It is important to note that even though the temperature bias is calculated using our new Mg/Ca-calcification temperature calibration, that equation is not necessarily applicable to the other size fractions and encrusted specimens. Calcite crust was suggested to have a different temperature dependency than primary calcite [*Bentov and Erez*, 2006] and, therefore, when different portions of calcite crust are present also different temperature dependencies would apply.

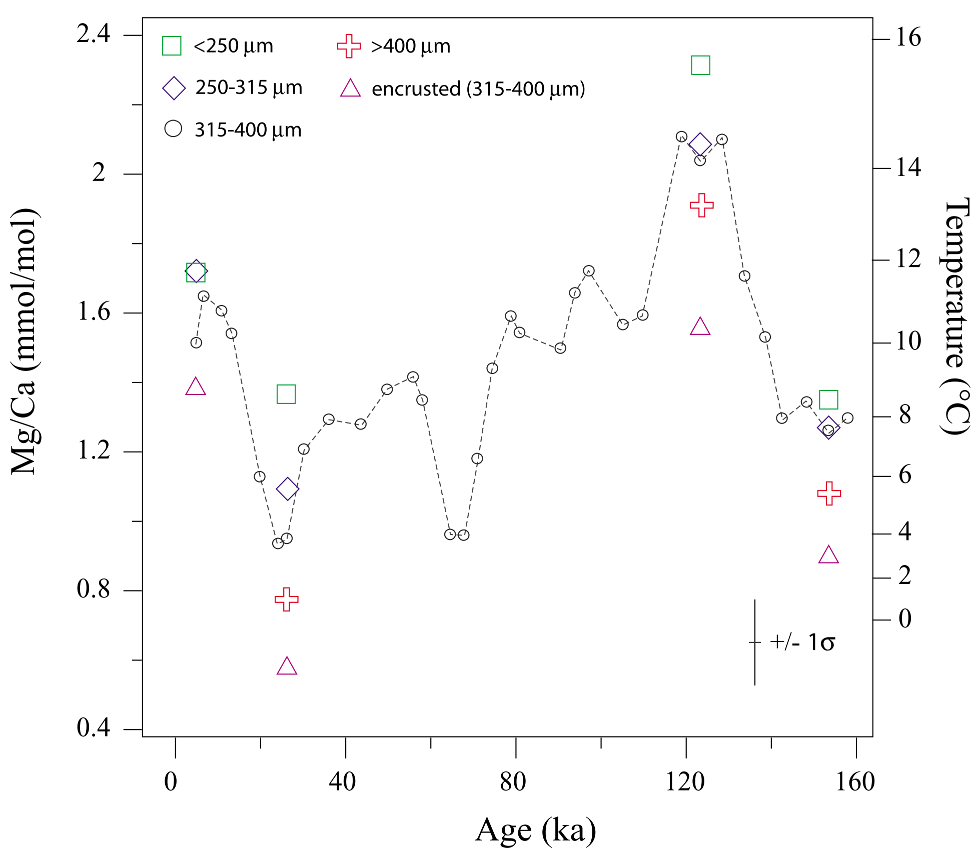

Figure 5. *G. inflata* Mg/Ca and temperatures for different size fractions (<250 μm, 250–315 μm, 315–400 μm, and >400 μm) of nonencrusted specimens and for encrusted specimens (315–400 μm) of gravity core PS2495-3, with the dashed line representing the downcore record determined on the 315–400 μm fraction. Analyses on more than one size fraction/encrustation stage were performed for the Holocene, MIS2, MIS5, and MIS6. The vertical black bar depicts the error (±1σ) associated with our Mg/Ca-calcification temperature calibration equation.

4.3. Downcore Record of PS2495-3: A Test Case Application

[26] In order to illustrate the application of our Mg/Ca-calcification temperature calibration of *G. inflata* as a recorder of permanent thermocline temperatures we established a downcore Mg/Ca record spanning the last two glacial-interglacial cycles for core PS2495-3 in the central South Atlantic (Figure 1a). This site has been the focus of several paleoceanographic studies [*Mackensen et al.*, 2001; *Gersonde et al.*, 2003, 2004] (Figure 4) providing a well-dated stratigraphic framework.

[27] Presently, core PS2495-3 is located within the SAZ. Data from the World Ocean Atlas show that there is a temperature gradient between the SAZ and the PFZ of ~5°C at 350–400 m water depth [*Locarnini et al.*, 2006]. The reconstructed temperature change at core PS2495-3 over Termination I is ~8°C (Figure 4). This value is similar to the one reconstructed for the sea surface based on foraminifera transfer functions [*Gersonde et al.*, 2004]. Temperature reconstructions for midlatitude South Atlantic sites not under the influence of migrating oceanic fronts show changes in SST over Termination I of 2–4°C [*Gersonde et al.*, 2003]. This suggests that an oceanic front migrated over our site during the Termination resulting in an additional 4–6°C temperature change. Therefore, our Mg/Ca temperature reconstruction shows that core PS2495-3 was located within the PFZ before Termination I and due to the southward migration of the SAF became under the influence of the SAZ at the end of Termination I.

[28] A marked difference between our record and the SST reconstructions from *Gersonde et al.* [2004] is that Mg/Ca temperatures show a clearly warmer MIS3 in comparison with MIS2 and MIS4 (Figure 4). The modern gradient of ~4°C between the sea surface and the permanent thermocline at our core site [*Locarnini et al.*, 2006], which was also found for the Holocene, MIS2, and MIS4, is absent during MIS3. As our reconstruction of *G. inflata* apparent calcification depth is constant throughout the South Atlantic it seems unlikely that this can be explained by a change in habitat depth. A meridional vertical profile of the water column shows that midlatitudinal fronts are present down to a water depth of 400–500 m with the boundary between warmer and colder waters deepening toward the north resulting in the modern temperature gradient (Figure 1b). But when the surface and the permanent thermocline were bathed in the same water mass the water column would have been less stratified. This could possibly explain the similar temperatures reconstructed for the sea surface and for the permanent thermocline during MIS3. We suggest that during MIS2 and MIS4 the permanent thermocline at our site was under the influence of the PFZ, and the surface under influence of the SAZ, whereas both were bathed by the SAZ during MIS3.

[29] Reconstructed permanent thermocline temperatures for MIS5 and MIS6 are significantly warmer (~4°C) than those reconstructed for the Holocene and MIS2, respectively (Figure 4). For MIS5 and MIS6 reconstructed temperatures based on Mg/Ca approach those reconstructed for the sea surface based on foraminifera transfer functions (Figure 4) [*Gersonde et al.*, 2004], possibly suggesting a less stratified water column. We hypothesize that the warmer temperatures recorded for the permanent thermocline at core PS2495-3 during MIS5 are related to a stronger influence of the Subtropical Zone (STZ) if compared to the Holocene. Likewise, the PFZ would not have extended as far north during MIS6 if compared to its northernmost extension during MIS2, leaving the permanent thermocline at core PS2495-3 under the influence of significantly warmer waters of the SAZ. The warmer conditions during MIS5 and MIS6 in the permanent thermocline therefore seem to point to a more southward position of the SAZ in the permanent thermocline rather than large changes at the surface.

[30] The reconstructed temperatures for MIS2 and MIS4 appear close to or even lower than the lowest temperature tolerated by *G. inflata* of ~3°C (Figure 5) [*Bé and Hutson*, 1977], and could have been caused by dissolution. Dissolution of biogenic carbonate in the water column or at the sediment-water interface preferentially dissolves higher-Mg portions of foraminiferal calcite [e.g., *Brown and Elderfield*, 1996]. As dissolution predominantly occurs in water masses undersaturated with respect to CO_3^{2-} [*Dekens et al.*, 2002; *Regenberg et al.*, 2006; *Mekik et al.*, 2007], deeper core locations are more easily affected by dissolution than shallower locations. At present core PS2495-3 is located in a water depth of only 3134 m and bathed by noncorrosive North Atlantic Deep Water and preservation is good. This is supported by Mg/Ca for *G. inflata* from a core top transect down to a water depth of 4000 m at the Rio Grande Rise which did not show any influence of dissolution [*Mekik et al.*, 2010]. But, we cannot exclude that during glacial time periods more corrosive Antarctic Bottom Water had some influence at the site. Reconstruction of the calcite lysocline based on ultastructural investigations of the planktonic foraminifer *G. bulloides* showed increased influence of Antarctic water masses throughout the South Atlantic during glacial periods [*Volbers and Henrich*, 2004]. This led to a general shoaling of the calcite lysocline toward ~3000 m water depth possibly causing some dissolution in our samples, and biasing Mg/Ca toward lower values. The correction of the Mg/Ca for dissolution would lead to an increase of 1–2°C [*Dekens et al.*, 2002; *Regenberg et al.*, 2006]. Thus, even corrected temperatures would still be significantly colder than MIS3.

[31] An alternative bias on the lowest temperatures of our downcore record could be related to the so-called cold-end effect of our calibration curve. This is a common feature of all Mg/Ca-temperature calibrations, both for planktonic and benthic foraminifera [*Martin and Lea*, 2002; *Meland et al.*, 2006; *Raitzsch et al.*, 2008]. Because small changes in Mg/Ca lead to large changes in temperature, slight differences in laboratory methods can have a significant effect on the reconstructed temperatures [*Rosenthal et al.*, 2004]. However, considering the procedure at our laboratory as well as the occurrence of adjacent samples with low Mg/Ca during both MIS2 and MIS4, we consider that the cold-end effect is probably not significant and the reconstructed pattern of temperature change is therefore most likely representative.

5. Conclusions

[32] We established a Mg/Ca-calcification temperature calibration for the deep-dwelling planktonic foraminifer *G. inflata* for the South Atlantic (from 8°S to 49°S) based on

a suite of 38 core top samples. Calcification temperatures were determined by comparing measured δ^{18}O of *G. inflata* with equilibrium δ^{18}O for calcite based on water column properties, resulting in an apparent calcification depth of 387 ± 179 m, reflecting permanent thermocline conditions, even under different upper water column structures. The resulting calibration equation is Mg/Ca = 0.72 ± 0.045/0.042 exp (0.076 ± 0.006 calcification temperature) (r^2 = 0.81) and covers the temperature range from 3.1°C to 16.5°C.

[33] Additionally, we compared the Mg/Ca signal of several size fractions and different encrustation states to evaluate the bias introduced to paleotemperature reconstructions by an indiscriminate selection of specimens. Differences of up to 7°C between the different forms emphasize the importance of careful selection of specimens when using *G. inflata* for paleoceanographic reconstructions.

[34] We tested our new calibration on low-resolution gravity core PS2495-3 from the Mid-Atlantic Ridge raised at 41°S, which is within the present-day SAZ, covering the last two glacial-interglacial cycles. Paleotemperatures show large changes of up to 8°C at Terminations I and II, as well as changes of 4–5°C over the transition into and out of MIS3. These large changes suggest that the migration of the STF and SAF over the core site was responsible for 4–6°C of the total observed temperature change. Accordingly, the permanent thermocline at our site is suggested to have been located within the STZ (MIS5), the SAZ (MIS1; MIS3; MIS6), and the PFZ (MIS2; MIS4). The reconstruction largely fits with SST reconstruction for the same site based on foraminifer transfer functions. These results show that *G. inflata* Mg/Ca is a reliable proxy to reconstruct paleotemperatures at permanent thermocline depths, being particularly useful for the reconstruction of the migration of midlatitudinal fronts.

[35] **Acknowledgments.** We thank M. Segl, P. Witte, S. Pape, and M. Kölling for technical support; B. Donner, J. Bijma, and A. Mackensen for providing samples; E. Hathorne, M. Mohtadi, and S. Steinke for discussion; D. Heslop for statistical support; and four anonymous reviewers and the Editor for their constructive comments. This study was funded by the DFG-Research Center/Excellence Cluster "The Oceans in the Earth System" via a Marum Fellowship to J. Groeneveld and the CNPq-Brazil Fellowship granted to C. M. Chiessi.

References

Anand, P., H. Elderfield, and M. H. Conte (2003), Calibration of Mg/Ca thermometry in planktonic foraminifera from a sediment trap time series, *Paleoceanography*, *18*(2), 1050, doi:10.1029/2002PA000846.

Barker, S., M. Greaves, and H. Elderfield (2003), A study of cleaning procedures used for foraminiferal Mg/Ca paleothermometry, *Geochem. Geophys. Geosyst.*, *4*(9), 8407, doi:10.1029/2003GC000559.

Bé, A. W. H., and W. H. Hutson (1977), Ecology of planktonic foraminifera and biogeographic patterns of life and fossil assemblages in the Indian Ocean, *Micropaleontology*, *23*, 369–414, doi:10.2307/1485406.

Bé, A. W. H., and D. S. Tolderlund (1971), Distribution and ecology of living planktonic foraminifera in surface waters of the Atlantic and Indian Oceans, in *The Micropaleontology of Oceans*, edited by B. M. Funnell and W. R. Riedel, pp. 105–149, Cambridge Univ. Press, London.

Bentov, S., and J. Erez (2006), Impact of biomineralization processes on the Mg content of foraminiferal shells: A biological perspective, *Geochem. Geophys. Geosyst.*, *7*, Q01P08, doi:10.1029/2005GC001015.

Berger, W. H. (1970), Planktonic foraminifera: Differential production and expatriation off Baja California, *Limnol. Oceanogr.*, *15*, 183–204, doi:10.4319/lo.1970.15.2.0183.

Bijma, J., W. W. Faber Jr., and C. Hemleben (1990), Temperature and salinity limits for growth and survival of some planktonic foraminifers in laboratory cultures, *J. Foraminiferal Res.*, *20*, 95–116, doi:10.2113/gsjfr.20.2.95.

Boltovskoy, D. (1994), The sedimentary record of pelagic biogeography, *Prog. Oceanogr.*, *34*, 135–160, doi:10.1016/0079-6611(94)90006-X.

Brown, S. J., and H. Elderfield (1996), Variations in Mg/Ca and Sr/Ca ratios of planktonic foraminifera caused by postdepositional dissolution: Evidence of shallow Mg-dependant dissolution, *Paleoceanography*, *11*, 543–551, doi:10.1029/96PA01491.

Came, R. E., D. W. Oppo, and J. F. McManus (2007), Amplitude and timing of temperature and salinity variability in the subpolar North Atlantic over the past 10 k.y, *Geology*, *35*, 315–318, doi:10.1130/G23455A.1.

Caron, D. A., O. R. Anderson, J. O. Lindsey, W. W. Faber Jr, and E. Lin Lim (1990), Effects of gametogenesis on test structure and dissolution of some spinose planktonic foraminifera and implications for test preservation, *Mar. Micropaleontol.*, *16*, 93–116, doi:10.1016/0377-8398(90)90031-G.

Chiessi, C. M., S. Ulrich, S. Mulitza, J. Pätzold, and G. Wefer (2007), Signature of the Brazil-Malvinas Confluence (Argentine Basin) in the isotopic composition of planktonic foraminifera from surface sediments, *Mar. Micropaleontol.*, *64*, doi:10.1016/j.marmicro.2007.02.002.

Chiessi, C. M., S. Mulitza, A. Paul, J. Pätzold, J. Groeneveld, and G. Wefer (2008), South Atlantic interocean exchange as the trigger for the Bølling warm event, *Geology*, *36*, 919–922, doi:10.1130/G24979A.1.

Cléroux, C., E. Cortijo, J.-C. Duplessy, and R. Zahn (2007), Deep-dwelling foraminifera as thermocline temperature recorders, *Geochem. Geophys. Geosyst.*, *8*, Q04N11, doi:10.1029/2006GC001474.

Cléroux, C., E. Cortijo, P. Anand, L. Labeyrie, F. Bassinot, N. Caillon, and J.-C. Duplessy (2008), Mg/Ca and Sr/Ca ratios in planktonic foraminifera: Proxies for upper water column temperature reconstruction, *Paleoceanography*, *23*, PA3214, doi:10.1029/2007PA001505.

Darling, K. F., and C. M. Wade (2008), The genetic diversity of planktic foraminifera and the global distribution of ribosomal RNA genotypes, *Mar. Micropaleontol.*, *67*, 216–238, doi:10.1016/j.marmicro.2008. 01.009.

Darling, K. F., M. Kucera, C. J. Pudsey, and C. M. Wade (2004), Molecular evidence links cryptic diversification in polar planktonic protists to Quaternary climate dynamics, *Proc. Natl. Acad. Sci. U. S. A.*, *101*, 7657–7662, doi:10.1073/pnas.0402401101.

de Vargas, C., L. Zaninetti, H. Hilbrecht, and J. Pawlowski (1997), Phylogeny and rates of molecular evolution of planktonic foraminifera: SSU rDNA sequences compared to the fossil record, *J. Mol. Evol.*, *45*, 285–294, doi:10.1007/PL00006232.

de Vargas, C., S. Renaud, H. Hilbrecht, and J. Pawlowski (2001), Pleistocene adaptive radiation in *Globorotalia truncatulinoides*: Genetic, morphologic, and environmental evidence, *Paleobiology*, *27*(1), 104–125, doi:10.1666/0094-8373(2001)027<0104:PARIGT>2.0.CO;2.

Dekens, P. S., D. W. Lea, D. K. Pak, and H. J. Spero (2002), Core top calibration of Mg/Ca in tropical foraminifera: Refining paleotemperature estimation, *Geochem. Geophys. Geosyst.*, *3*(4), 1022, doi:10.1029/2001GC000200.

Deuser, W. G., and E. H. Ross (1989), Seasonally abundant planktonic foraminifera of the Sargasso Sea–Succession, deep-water fluxes, isotopic composition and paleoceanographic implication, *J. Foraminiferal Res.*, *19*, 268–293, doi:10.2113/gsjfr.19.4.268.

Dürkoop, A. (1998), Der Brasil-Strom im Spätquartär: Rekonstruktion der oberflächennahen Hydrographie während der letzten 400 000 Jahre, *Ber. Fachbereich Geowiss. 119*, 121 pp., Bremen Univ., Bremen, Germany.

Elderfield, H., and G. Ganssen (2000), Past temperature and δ^{18}O of surface ocean waters inferred from foraminiferal Mg/Ca ratios, *Nature*, *405*, 442–445, doi:10.1038/35013033.

Fairbanks, R. G., M. Sverdlove, R. Free, P. H. Wiebe, and A. W. H. Bé (1982), Vertical distribution and isotopic fractionation of living planktonic foraminifera from the Panama Basin, *Nature*, *298*, 841–844, doi:10.1038/298841a0.

Ferguson, J. E., G. M. Henderson, M. Kucera, and R. E. M. Rickaby (2008), Systematic change of foraminiferal Mg/Ca ratios across a strong salinity gradient, *Earth Planet. Sci. Lett.*, *265*, 153–166, doi:10.1016/j.epsl.2007.10.011.

Gersonde, R., et al. (2003), Last glacial sea surface temperatures and sea-ice extent in the Southern Ocean (Atlantic-Indian sector): A multiproxy approach, *Paleoceanography*, *18*(3), 1061, doi:10.1029/2002PA000809.

Gersonde, R., A. Abelmann, G. Cortese, S. Becquey, C. Bianchi, U. Brathauer, H.-S. Niebler, U. Zielinski, and J. Pätzold (2004), The late Pleistocene south Atlantic and southern ocean surface–A summary of time-series studies, in *The South Atlantic in the Late Quaternary: Reconstruction of Material Budgets and Current Systems*, edited by G. Wefer, S. Mulitza, and V. Ratmeyer, pp. 499–529, Springer, Berlin.

Greaves, M., et al. (2008), Interlaboratory comparison study of calibration standards for foraminiferal Mg/Ca thermometry, *Geochem. Geophys. Geosyst.*, *9*, Q08010, doi:10.1029/2008GC001974.

Groeneveld, J., D. Nürnberg, R. Tiedemann, G.-J. Reichart, S. Steph, L. Reuning, D. Crudeli, and P. Mason (2008), Foraminiferal Mg/Ca increase in the Caribbean during the Pliocene: Western Atlantic Warm Pool formation, salinity influence, or diagenetic overprint?, *Geochem. Geophys. Geosyst.*, *9*, Q01P23, doi:10.1029/2006GC001564.

Harloff, J., and A. Mackensen (1997), Recent benthic foraminiferal associations and ecology of the Scotia Sea and Argentine Basin, *Mar. Micropaleontol.*, *31*, 1–29, doi:10.1016/S0377-8398(96)00059-X.

Hathorne, E. C., R. H. James, and R. S. Lampitt (2009), Environmental versus biomineralization controls on the intratest variation in the trace element composition of the planktonic foraminifera *G. inflata* and *G. scitula*, *Paleoceanography*, *24*, PA4204, doi:10.1029/2009PA001742.

Hoogakker, B. A. A., G. P. Klinkhammer, H. Elderfield, E. J. Rohling, and C. Hayward (2009), Mg/Ca paleothermometry in high salinity environments, *Earth Planet. Sci. Lett.*, *284*, 583–589, doi:10.1016/j.epsl.2009.05.027.

Kennett, J. P., and M. S. Srinivasan (1983), *Neogene Planktonic Foraminifera: A Phylogenetic Atlas*, Hutchinson Ross, Stroudsburg, Pa.

Kisakürek, B., A. Eisenhauer, F. Böhm, D. Garbe-Schönberg, and J. Erez (2008), Controls on shell Mg/Ca and Sr/Ca in cultured planktonic foraminifera, *Globigerinoides ruber* (white), *Earth Planet. Sci. Lett.*, *273*, 260–269, doi:10.1016/j.epsl.2008.06.026.

Lea, D. W., T. A. Mashiotta, and H. J. Spero (1999), Controls on magnesium and strontium uptake in planktonic foraminifera determined by live culturing, *Geochim. Cosmochim. Acta*, *63*, 2369–2379, doi:10.1016/S0016-7037(99)00197-0.

LeGrande, A. N., and G. A. Schmidt (2006), Global gridded data set of the oxygen isotopic composition in seawater, *Geophys. Res. Lett.*, *33*, L12604, doi:10.1029/2006GL026011.

Lisiecki, L. E., and M. E. Raymo (2005), A Pliocene-Pleistocene stack of 57 globally distributed benthic $\delta^{18}O$ records, *Paleoceanography*, *20*, PA1003, doi:10.1029/2004PA001071.

Locarnini, R. A., A. V. Mishonov, J. I. Antonov, T. P. Boyer, and H. E. Garcia (2006), *World Ocean Atlas 2005*, vol. 1, *Temperature*, *NOAA Atlas NESDIS*, vol. 61, edited by S. Levitus, 182 pp., NOAA, Silver Spring, Md.

Lončarić, N., F. J. C. Peeters, D. Kroon, and G.-J. A. Brummer (2006), Oxygen isotope ecology of recent planktic foraminifera at the central Walvis Ridge (SE Atlantic), *Paleoceanography*, *21*, PA3009, doi:10.1029/2005PA001207.

Mackensen, A., M. Rudolph, and G. Kuhn (2001), Late Pleistocene deep-water circulation in the subantarctic eastern Atlantic, *Global Planet. Change*, *30*, 197–229, doi:10.1016/S0921-8181(01)00102-3.

Martin, P. A., and D. W. Lea (2002), A simple evaluation of cleaning procedures on fossil benthic foraminiferal Mg/Ca, *Geochem. Geophys. Geosyst.*, *3*(10), 8401, doi:10.1029/2001GC000280.

Mashiotta, T. A., D. W. Lea, and H. J. Spero (1999), Glacial-interglacial changes in Subantarctic sea surface temperature and $\delta^{18}O$-water using foraminiferal Mg, *Earth Planet. Sci. Lett.*, *170*, 417–432, doi:10.1016/S0012-821X(99)00116-8.

McKenna, V. S., and W. L. Prell (2004), Calibration of the Mg/Ca of *Globorotalia truncatulinoides* (right) for the reconstruction of marine temperature gradients, *Paleoceanography*, *19*, PA2006, doi:10.1029/2000PA000604.

Mekik, F., R. Francois, and M. Soon (2007), A novel approach to dissolution correction of Mg/Ca–based paleothermometry in the tropical Pacific, *Paleoceanography*, *22*, PA3217, doi:10.1029/2007PA001504.

Mekik, F., N. Noll, and M. Russo (2010), Progress toward a multi-basin calibration for quantifying deep sea calcite preservation in the tropical/subtropical world ocean, *Earth Planet. Sci. Lett.*, *299*, 104–117, doi:10.1016/j.epsl.2010.08.024.

Meland, M. Y., E. Jansen, H. Elderfield, T. M. Dokken, A. Olsen, and R. G. J. Bellerby (2006), Mg/Ca ratios in the planktonic foraminifer *Neogloboquadrina pachyderma* (sinistral) in the northern North Atlantic/Nordic Seas, *Geochem. Geophys. Geosyst.*, *7*, Q06P14, doi:10.1029/2005GC001078.

Mollenhauer, G., J. F. McManus, A. Benthien, P. J. Müller, and T. I. Eglinton (2006), Rapid lateral particle transport in the Argentine Basin: Molecular ^{14}C and $^{230}Th_{xs}$ evidence, *Deep Sea Res., Part I*, *53*, 1224–1243, doi:10.1016/j.dsr.2006.05.005.

Mulitza, S., D. Boltovskoy, B. Donner, H. Meggers, A. Paul, and G. Wefer (2003), Temperature:$\delta^{18}O$ relationships of planktonic foraminifera collected from surface waters, *Palaeogeogr. Palaeoclimatol. Palaeoecol.*, *202*, 143–152, doi:10.1016/S0031-0182(03)00633-3.

Niebler, H.-S., and R. Gersonde (1998), A planktic foraminiferal transfer function for the southern South Atlantic Ocean, *Mar. Micropaleontol.*, *34*, 213–234, doi:10.1016/S0377-8398(98)00009-7.

Nürnberg, D., and J. Groeneveld (2006), Pleistocene variability of the Subtropical Convergence at East Tasman Plateau: Evidence from planktonic foraminiferal Mg/Ca (ODP Site 1172A), *Geochem. Geophys. Geosyst.*, *7*, Q04P11, doi:10.1029/2005GC000984.

Nürnberg, D., J. Bijma, and C. Hemleben (1996), Assessing the reliability of magnesium in foraminiferal calcite as a proxy for water mass temperatures, *Geochim. Cosmochim. Acta*, *60*, 803–814, doi:10.1016/0016-7037(95)00446-7.

Nürnberg, D., A. Müller, and R. R. Schneider (2000), Paleo-sea surface temperature calculations in the equatorial east Atlantic from Mg/Ca ratios in planktic foraminifera: A comparison to sea surface temperature estimates from U_k^{37}, oxygen isotopes, and foraminiferal transfer function, *Paleoceanography*, *15*, 124–134, doi:10.1029/1999PA000370.

Olson, D. B., G. P. Podestá, R. H. Evans, and O. B. Brown (1988), Temporal variations in the separation of Brazil and Malvinas Currents, *Deep Sea Res., Part A*, *35*, 1971–1990, doi:10.1016/0198-0149(88)90120-3.

Peterson, R. G., and L. Stramma (1991), Upper-level circulation in the South Atlantic Ocean, *Prog. Oceanogr.*, *26*, 1–73, doi:10.1016/0079-6611(91)90006-8.

Raitzsch, M., H. Kuhnert, J. Groeneveld, and T. Bickert (2008), Benthic foraminifer Mg/Ca anomalies in South Atlantic core top sediments and their implications for paleothermometry, *Geochem. Geophys. Geosyst.*, *9*, Q05010, doi:10.1029/2007GC001788.

Regenberg, M., D. Nürnberg, S. Steph, J. Groeneveld, D. Garbe-Schönberg, R. Tiedemann, and W. Dullo (2006), Assessing the effect of dissolution on planktonic foraminiferal Mg/Ca ratios: Evidence from Caribbean core tops, *Geochem. Geophys. Geosyst.*, *7*, Q07P15, doi:10.1029/2005GC001019.

Regenberg, M., S. Steph, D. Nürnberg, R. Tiedemann, and D. Garbe-Schönberg (2009), Calibrating Mg/Ca ratios of multiple planktonic foraminiferal species with $\Delta^{18}O$-calcification temperatures: Paleothermometry for the upper water column, *Earth Planet. Sci. Lett.*, *278*, 324–336, doi:10.1016/j.epsl.2008.12.019.

Rosenthal, Y., et al. (2004), Interlaboratory comparison study of Mg/Ca and Sr/Ca measurements in planktonic foraminifera for paleoceanographic research, *Geochem. Geophys. Geosyst.*, *5*, Q04D09, doi:10.1029/2003GC000650.

Sadekov, A., S. M. Eggins, P. De Deckker, U. Ninnemann, W. Kuhnt, and F. Bassinot (2009), Surface and subsurface seawater temperature reconstruction using Mg/Ca microanalysis of planktonic foraminifera *Globigerinoides ruber, Globigerinoides sacculifer*, and *Pulleniatina obliquiloculata*, *Paleoceanography*, *24*, PA3201, doi:10.1029/2008PA001664.

Schmidt, M. W., H. J. Spero, and D. W. Lea (2004), Links between salinity variation in the Caribbean and North Atlantic thermohaline circulation, *Nature*, *428*, 160–163, doi:10.1038/nature02346.

Shackleton, N. J. (1974), Attainment of isotope equilibrium between ocean water and the benthonic foraminiferal genus *Uvigerina*: Isotopic changes in the ocean during the last glacial, *Colloq. Int. Cent. Natl. Rech. Sci.*, *219*, 203–209.

Steinke, S., H.-Y. Chiu, P.-S. Yu, C.-C. Shen, H. Erlenkeuser, L. Löwemark, and M.-T. Chen (2006), On the influence of sea level and monsoon climate on the southern South China Sea freshwater budget over the last 22,000 years, *Quat. Sci. Rev.*, *25*, 1475–1488, doi:10.1016/j.quascirev.2005.12.008.

Stramma, L., and M. England (1999), On the water masses and mean circulation of the South Atlantic Ocean, *J. Geophys. Res.*, *104*, 20,863–20,883, doi:10.1029/1999JC900139.

Tsuchiya, M., L. D. Talley, and M. S. McCartney (1994), Water-mass distributions in the western South Atlantic; A section from South Georgia Island (54S) northward across the equator, *J. Mar. Res.*, *52*, 55–81, doi:10.1357/0022240943076759.

Volbers, A. N. A., and R. Henrich (2004), Calcium carbonate corrosiveness in the South Atlantic during the Last Glacial Maximum as inferred from changes in the preservation of *Globigerina bulloides*: A proxy to determine deep-water circulation patterns?, *Mar. Geol.*, *204*, 43–57, doi:10.1016/S0025-3227(03)00372-4.

Wilke, I., T. Bickert, and F. J. C. Peeters (2006), The influence of seawater carbonate ion concentration $[CO_3^{2-}]$ on the stable carbon isotope composition of the planktic foraminifera species *Globorotalia inflata*, *Mar. Micropaleontol.*, *58*, 243–258, doi:10.1016/j.marmicro.2005.11.005.

C. M. Chiessi, School of Arts, Sciences and Humanities, University of São Paulo, Av. Arlindo Bettio 1000, CEP03828-000 São Paulo SP, Brazil.

J. Groeneveld, Marum Excellence Cluster, Alfred Wegener Institute for Polar and Marine Research, Columbusstrasse, D-27568 Bremerhaven, Germany. (jeroen.groeneveld@awi.de)